

Wide band X-ray Imager (W XI) and Soft Gamma-ray Detector (SGD) for the NeXT Mission

T. Takahashi^{a,b}, A. Awaki^f, T. Dotani^f, Y. Fukazawa^d, K. Hayashida^e, T. Kamae^f,
 J. Kataoka^g, N. Kawabata^f, S. Kitamoto^h, T. Kohmuraⁱ, M. Kokubun^b, K. Koyama^j,
 K. Makishima^b, H. Matsumoto^j, E. Miyata^e, T. Murakami^k, K. Nakazawa^a, M. Nomachi^e,
 M. Ozaki^f, H. Tajima^f, M. Tashiro^l, T. Tamagawa^m, Y. Terada^m, H. Tsunemi^f, T. Tsuru^j,
 K. Yamaguchiⁿ, D. Yonetoku^k, and A. Yoshidaⁿ

^aInstitute of Space and Astronautical Science, JAXA, Sagamihara, Kanagawa, 229-8510, Japan;

^bDepartment of Physics, University of Tokyo, Bunkyo-ku, Tokyo, 113-0033, Japan;

^cDepartment of Physics, Ehime University, Matsuyama, Ehime, 790-8577, Japan;

^dDepartment of Physics, Hiroshima University, Higashi-Hiroshima, Hiroshima, 739-8526, Japan;

^eDepartment of Physics, Osaka University, Toyonaka, Osaka, 560-0043, Japan;

^fStanford Linear Accelerator Center, Stanford, CA 94309-4349, USA;

^gDepartment of Physics, Tokyo Institute of Technology, Meguro-ku, Tokyo, 152-8551, Japan;

^hDepartment of Physics, Rikkyo University, Toshima-ku, Tokyo, 171-8501, Japan;

ⁱDepartment of Physics, Kogakuin University, Hachioji, Tokyo, 192-0015, Japan;

^jDepartment of Physics, Kyoto University, Sakyo-ku, Kyoto, 606-8502, Japan;

^kDepartment of Physics, Kanazawa University, Kanazawa, Ishikawa, 920-1192, Japan;

^lDepartment of Physics, Saitama University, Saitama, 338-8570, Japan;

^mRIKEN, Wako, Saitama, 351-0198, Japan;

ⁿDepartment of Physics, Aoyama Gakuin University, Sagamihara, Kanagawa, 229-8551, Japan

ABSTRACT

The NeXT mission has been proposed to study high-energy non-thermal phenomena in the universe. The high-energy response of the super mirror will enable us to perform the first sensitive imaging observations up to 80 keV. The focal plane detector, which combines a fully depleted X-ray CCD and a pixellated CdTe detector, will provide spectra and images in the wide energy range from 0.5 keV to 80 keV. In the soft gamma-ray band up to 1 MeV, a narrow field-of-view Compton gamma-ray telescope utilizing several tens of layers of thin Si or CdTe detector will provide precise spectra with much higher sensitivity than present instruments. The continuum sensitivity will reach several 10^8 photons/s/keV/cm² in the hard X-ray region and a few 10^7 photons/s/keV/cm² in the soft-ray region.

Key words: Hard X-ray, gamma-ray, X-ray Astronomy, Gamma-ray Astronomy, CdTe, Compton Camera

1. INTRODUCTION

The hard X-ray and gamma-ray bands have long been recognized as important windows for exploring the energetic universe. It is in these energy bands that non-thermal emission, primarily due to accelerated high energy particles, becomes dominant. However, by comparison with the soft X-ray band, where the spectacular data from the XMM-Newton and Chandra satellites are revolutionizing our understanding of the high-energy universe, the sensitivities of hard X-ray missions, even so far, or currently under construction, have not dramatically improved over the last decade. In order to study the energy content of non-thermal emission and to draw a more complete picture of the non-thermal universe, observations by highly sensitive missions are important.

Further author information: (Send correspondence to T. Takahashi) E-mail: takahashi@astro.isas.jaxa.jp

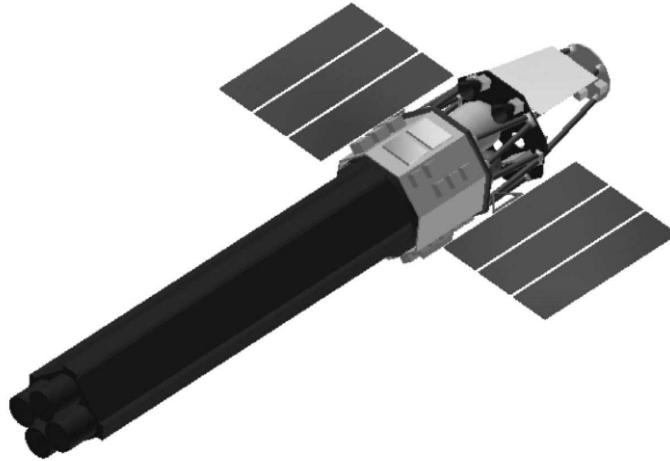


Figure 1. An artist's drawing of the NeXT satellite. The focal length of the HXT is 12 m.

The NeXT (Non-thermal Energy Exploration Telescope) mission proposed in Japan is a successor to the Astro-E2 mission, and is optimized to study the high-energy non-thermal universe (Fig.1).^{1,2} NeXT will carry three hard X-ray telescopes (HXTs) for the wide band X-ray imager (W XI), one soft X-ray telescope (SXT) for the soft X-ray spectrometer (SXS), and a soft -ray detector (SGD). With the first imaging observations up to 80 keV, NeXT is expected to achieve two orders of magnitude improvement in the sensitivity in the hard X-ray region. The SGD utilizes a new concept of a narrow-FOV Compton telescope^{3,4} to improve the sensitivity in the soft -ray region for matching with the sensitivity of the HXT/W XI combination. The extremely low background brought by the SGD will allow us to measure the precise -ray spectrum up to 1 MeV. Furthermore, as described in the separate paper,⁵ the SGD will be sensitive to the polarization of the incident -rays, and will potentially be the first hard X-ray polarimeter in orbit. In addition to these high energy instruments, the soft X-ray spectrometer (SXS) will map out the velocity field in objects by means of X-ray line profiles. The SXS is based on a transition edge sensor (TES) and has both spectral and spatial resolution much better than the X-ray calorimeter (XRS) onboard the Astro-E2.⁶ In this paper, we describe the current ideas about the W XI and the SGD.

2. WIDE-BAND X-RAY IMAGER (W XI)

The non-imaging instruments known so far were essentially limited to studies of sources with 10-100 keV fluxes of at best $> 10^{-12}$ - 10^{-11} erg cm⁻² s⁻¹. This limitation is due to the presence of high un-rejected backgrounds from particle events and Cosmic X-ray radiation, which increasingly dominate above 10 keV. Imaging, and especially focusing instruments have two tremendous advantages: first, the volume of the focal plane detector can be made much smaller than for non-focusing instruments, and second, the residual background, often time-variable, can be measured simultaneously with the source, and can be reliably subtracted.

A depth-graded multi-layer mirror, referred to as a super mirror, reflects X-rays not only by total external reflection but also by Bragg reflection. A super mirror consists of a stack of multi-layers with different sets of periodic length and number of layer pairs. The current mirror design of the HXT for NeXT^{7,8} is based on a carbon/platinum coating, which is adopted in the InFOCUS project by Nagoya University and NASA's GSFC.⁹ With three HXT units, effective areas of 1100 cm² at 20 keV and 230 cm² at 60 keV can be achieved with a focal length of 12 m.¹ Fig. 2 compare the effective area of the three HXTs with XMM-Newton and Astro-E2. The effective area of the Soft X-ray Telescope (SXT) and the SGD are also shown in the figure.

In order to match the energy range covered by the super mirror (0.5 - 80 keV), the focal plane detector is required to cover a very wide energy band. To this end, we have proposed a new focal plane detector based on

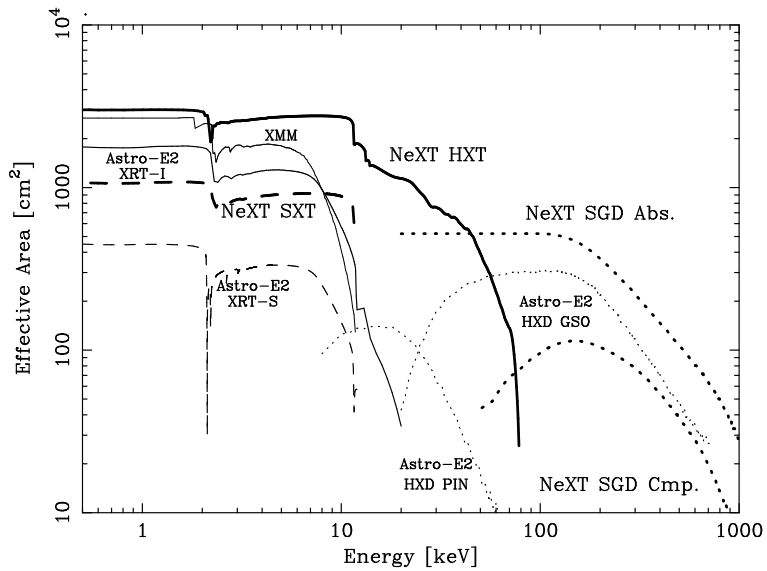


Figure 2. Effective area of the HXT and the SXT as compared to XMM/Newton and Astro-E2. Effective area of the gamma-ray detectors are also shown for the HXD/Astro-E2 and the SGD/NeXT.

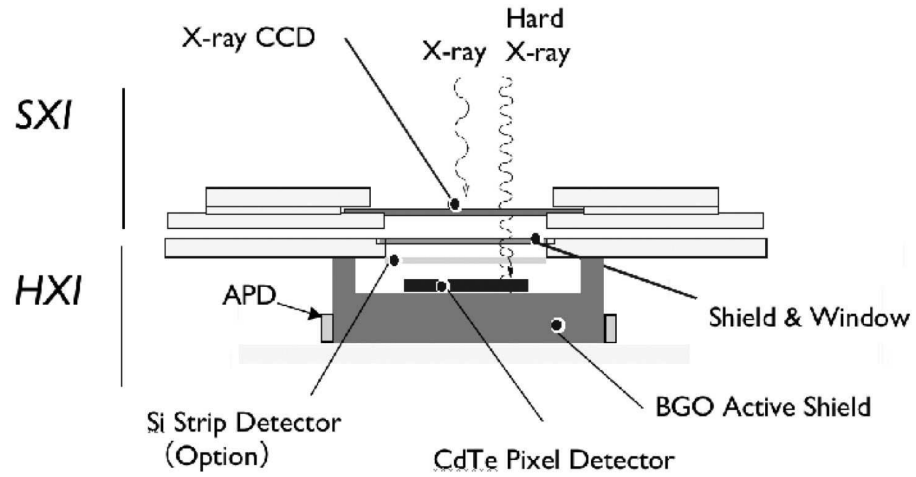


Figure 3. Conceptual drawing of the WXI proposed for the NeXT mission. The WXI is composed of two sub-instruments: the soft X-ray imager (SXI) and the hard X-ray imager (HXI). The CdTe pixel detector in the HXI is placed beneath the X-ray CCD in the SXI. In the WXI, soft X-rays are absorbed in the CCD, while hard X-rays penetrate through the CCD and are absorbed in the CdTe pixel detector. The Si strip detector is considered as an option to shield fluorescence lines from CdTe.

Table 1. Specification for the HXI and the SXI

HXI	Energy Range	8 { 80 keV
	Energy Resolution	0.5 { 1 keV (FWHM)
	Trigger Threshold	8 keV
	Pixel Size	200 { 500 μ m
	Detector Size	20 mm { (20 { 30) mm
	Timing Resolution	< 100 μ s
Operating Temperature		50 { 0 degree
SXI	Energy Range	0.5 { 20 keV
	Energy Resolution	130 eV (FWHM at 6keV)
	Pixel Size	27 { 27 μ m ²
	Detector Size	42 mm { 42 mm
	Operating Temperature	

an idea of combining a fully depleted CCD and a CdTe (Cadmium Telluride) pixel detector^{3,10} as the WXI.^{11,12} Figure 3 is a schematic design of the WXI showing the concept. The WXI is composed of two sub-instruments; the soft X-ray imager (SXI) and the hard X-ray imager (HXI). Specifications of the SXI and the HXI are listed in Table 1. The SXI is based on an X-ray CCD with very thin dead layer in the device and the HXI is based on a fine-pitch CdTe pixel detector. In the WXI, soft X-rays will be absorbed in the CCD, while hard X-rays will penetrate through the CCD and be absorbed in the CdTe pixel detector. Semiconductor detectors with high mass absorption coefficient, such as CdTe, are crucial for the detection of hard X-ray photons. For CdTe, even a detector with a thickness of 0.5 mm provides a good detection efficiency for the hard X-ray region covered by the HXI. As shown in Fig. 3, the CdTe detector mounted in the HXI is shielded by a BGO ($\text{Bi}_4\text{Ge}_3\text{O}_{12}$) scintillator. This shield is indispensable, as the non X-ray background is the dominant source of the background in the energy range of the HXI. A thickness of 2 cm for BGO will be required, not only for shielding against background photons but also for reducing the number of particles that reach the CdTe detector and give rise to activation.

The SXI detects soft X-rays below 10-20 keV with the high position resolution of 27 μ m. It will be based on the technology which has been accumulated for the Japanese MAXI mission.¹³ The SXI utilizes a single, large-format CCD which covers 12 { 12 arc min² at the focal plane. An energy resolution of 130 eV (FWHM) at 6 keV is expected at the operating temperature of 90 deg. SXI utilizes a thinned CCD, whose undepleted layer is largely removed. This is necessary to make it transparent to hard X-rays. If we adopt a backside-illuminated CCD, no extra process is necessary as the undepleted layer is already removed. The CCD support and cooling structures are configured near the rim of the CCD so as not to interfere with the transmission of hard X-rays. Thus the transparent portion to hard X-rays is smaller than the size of the CCD itself. In order further to reduce the undepleted layer and to improve the high energy response, the development of fully depleted p-channel CCD fabricated on n-type high-resistivity silicon is now under way.¹⁴

The current goal for the CdTe detector in the HXI is a pixel detector with both a fine position resolution of 200 { 250 μ m and a high energy resolution better than 1 keV (FWHM), in the energy range from 5 keV to 80 keV. Since significant progress has been made recently on the development of CdTe technologies,¹⁵ it is now possible to fabricate a single crystal CdTe device with the size of 2 { 2 cm². Signals from the individual pixel electrodes formed on the surface of the CdTe wafer are fed into the readout circuit built in the ASIC. To realize the fine pitch CdTe pixel detector for the HXI, a low noise front-end ASIC with more than several thousand independent channels will be the key technology. Development of a simple and robust connection technology is also necessary, because high compression and/or high ambient temperature would damage the CdTe. In order to cooperate with the BGO shield, the detector should have fast timing resolution of 10 to 100 μ s, such that we can veto the events when there is a hit in the shield. Taking these requirements into consideration, we have been working on high performance CdTe detectors for both planar and pixel configuration.^{16,17} Based on the CdTe wafers manufactured from the single crystal grown by the Traveling Heater Method (THM-CdTe) and with the

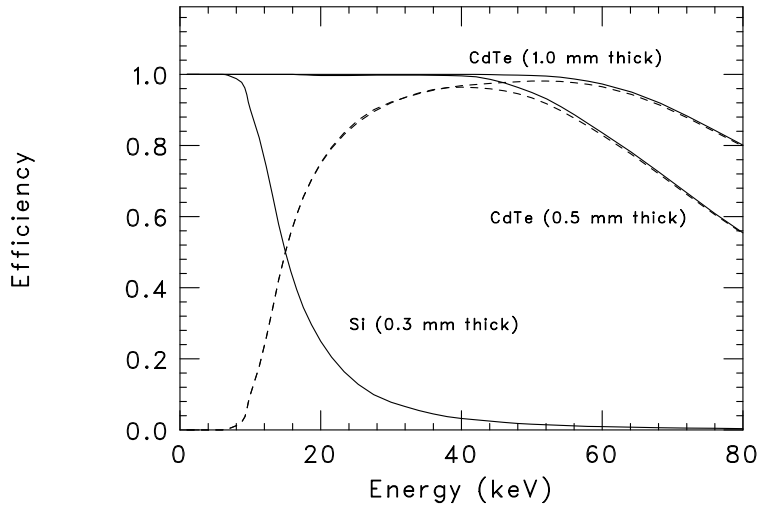


Figure 4. Efficiency of the SXI with 300 μm thick Si CCD and the HXI for 0.5 mm and 1.0 mm thick CdTe detector. Effects of a possible dead layer in the Si CCD are not included in the calculation.

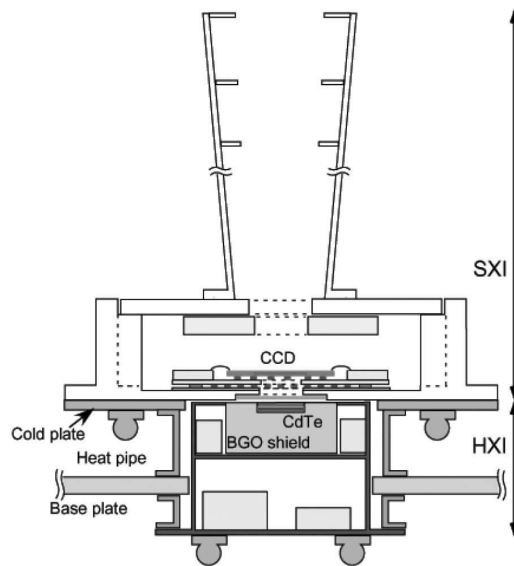


Figure 5. Schematic drawing of the W X I. The SX I and the H X I will be operated at different temperatures.

technology for gold-stud bump bonding, we have developed CdTe detectors with high energy resolution.^{18,19}

With NeXT, we expect to achieve an area of about 750 cm² at 30 keV with a typical angular resolution of 30". Fig. 4 shows the efficiency of the W X I with a 300 μm thick X-ray CCD and a 0.5 or 1.0 mm CdTe pixel detector. In the calculation, effects of a possible dead layer in the CCD are not taken into account. By assuming a background level of 1 × 10⁴ counts/s/cm²/keV, in which a non X-ray background is dominant, the source detection limit in 100 ksec would be roughly 10¹⁴ erg cm² s⁻¹ in terms of the 10–80 keV flux for a power-law spectrum with a photon index of 2. This is about two orders of magnitude better than present instrumentation.

Table 2. Specification of the SGD¹

SGD	Energy Range	10 keV { 1 M eV
	Energy Resolution	2 keV (FWHM, 40 keV)
	Geometrical Area	625 cm ²
	Effective Area	525 cm ² (100 keV)
		110 cm ² (500 keV)
		100 cm ² (Compton mode, 100 keV)
		40 cm ² (Compton mode, 500 keV)
	Opening Angle	0.6 - 0.6 deg ² (< 100 keV)
		4 - 4 deg ² (> 100 keV)
	(Angular Resolution)	1.5 deg (RMS, Compton mode, 500 keV)
	Operating Temperature	20 { 0 degree

Table 3. Specification of the DSSD and the CdTe pixel detector for the SGD¹

DSSD	strip pitch	0.4 mm
	thickness	0.5 mm
	number of strips	125
	active area	5 - 5 cm ²
	energy resolution	1.5 keV (FWHM)
CdTe pixel detectors	pixel size	2 - 2 mm ²
	thickness	0.5 mm (thin), 5 mm (thick)
	number of pixels	25 - 25
	active area	5 - 5 cm ²
	energy resolution	1.5 keV (FWHM)

3. NARROW FOV COMPTON TELESCOPE

Highly sensitive observations in the energy range above the HXT/WXIBandpass is crucial to study the spectrum of accelerated particles. The SGD outperform s previous soft- γ instruments in background rejection capability by adopting a new concept of narrow-FOV Compton telescope.^{3,4,11} In the energy range above one hundred keV (sub-MeV region), shielding against background photons becomes important yet difficult. The well-type phoswich counter, which we developed for the WELCOME balloon experiment^{20,21} and also for the Astro-E Hard X-ray Detector (HXD)^{22,26} is a possible solution to achieve a very low background rate. The phoswich configuration and a tight and active "well-type" shield made of BGO scintillators is expected to reduce the background to $< 10^{-4}$ counts/cm²/s/keV, almost the limit achieved by the configuration of active shield and collimator.

In order to lower the background dramatically and thus to improve the sensitivity as compared to the HXD, we combine a stack of Si strip detectors and CdTe pixel detectors to form a Compton telescope. The telescope is then mounted inside the bottom of a well-type active shield. As shown schematically in Fig.6, the telescope consists of 24 layers of DSSDs (double-sided silicon strip detectors) and 2 layers of thin CdTe pixellated detectors surrounded by 5 mm thick CdTe pixellated detectors. Specifications for the SGD and for each component for the Compton telescope are listed in Table 2 and Table 3, respectively. The opening angle provided by the BGO shield is 4 degree at 500 keV. As compared to the HXD, the shield part is made compact by adopting the newly developed avalanche photodiode.^{27,28} An additional copper collimator restricts the field of view of the telescope to 30' for low energy photons (< 100 keV) to minimize the flux due to the Cosmic X-ray Background from the FOV. These modules are then arrayed to provide the required area (Figure 7). Figure 8 shows a drawing of the design goal of the SGD instrument which consists of a 5 x 5 array of identical detector modules.

An important feature of the SGD is that we can require each event to interact twice in the stacked detector, once by Compton scattering in a stack of Si strip detectors, and then by photo-absorption in the CdTe part

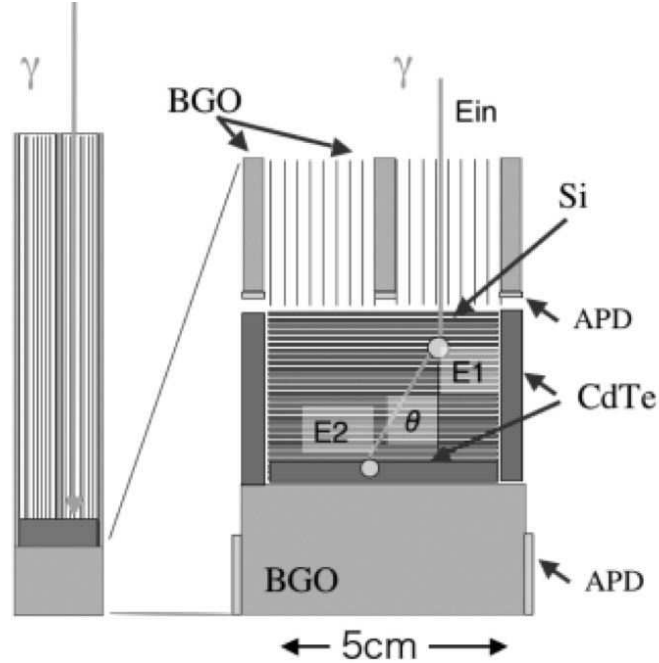


Figure 6. Conceptual design of the SGD module. A stack of 24 SiD SSDs and CdTe pixel detectors are assembled to form a semiconductor Compton Telescope. The telescope is mounted inside the bottom of a well-type active shield. The opening angle provided by the BGO shield is 4 deg at 500 keV. An additional copper collimator restricts the field of view of the telescope to 30° for low energy photons (< 100 keV). With this narrow FOV, events are rejected as background, if the reconstructed Compton ring does not intercept the FOV.

(Compton mode). Once the locations and energies of the two interactions are measured, the Compton kinematics allows us to calculate the energy and direction (as a cone in the sky) of the incident γ -ray by following the Compton equation,

$$E_{in} = E_1 + E_2; \quad (1)$$

$$\cos \theta = 1 - m_e c^2 \left(\frac{1}{E_2} - \frac{1}{E_1 + E_2} \right); \quad (2)$$

where E_1 is the energy of the recoil electron, E_2 is the energy of the scattered photon and θ is the scattering angle. The high spectral and spatial resolution of Si and CdTe semiconductor detectors allow the instrument to achieve high angular resolution. Since the major interaction of photon above 60 keV in Si is Compton scattering, the stack of DSSDs acts as an efficient scatterer especially for the low energy region below 300 keV. Regarding the uncertainty of the order of scattering in an event, we can use the relation that the energy deposition by Compton scattering is always smaller than that of the photo-absorption for energies below $E = 255 \text{ keV}$ ($E = m_e/2$). This relation holds above this energy, if the scattering angle is smaller than $\cos^{-1} \left(1 - \frac{1}{2} \frac{m_e}{E} \right)$.¹¹

The major advantage of employing a narrow FOV is that the direction of incident γ -rays is constrained inside the FOV. If the Compton ring does not intercept the FOV, we can reject the event as background. Most backgrounds can be rejected by requiring this condition (albeit with an corresponding reduction in instrument effective area). Background photons from the BGO and copper collimator for which the reconstructed Compton ring intersects the FOV, cannot be eliminated if there is no signal detected in the active shield, however this source of background contributes only within a limited range of scattering angle. Combining background suppression techniques available in the SGD, we expect to achieve background levels of 5×10^{-7} counts/s/cm²/keV at 100 keV and 2×10^{-7} counts/s/cm²/keV at 500 keV. As shown in Fig. 2, the effective area of the SGD in the Compton mode is 120 cm² at 200 keV and 50 cm² at 400 keV, if we use 25 units (total geometrical area is 625 cm²).

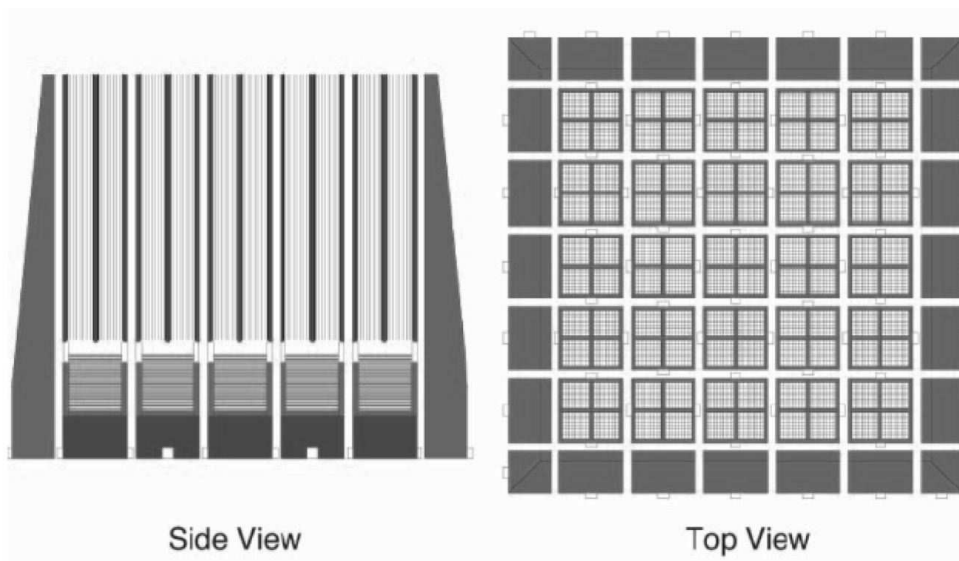


Figure 7. A schematic drawing of the SGD. It consists of 25 units of the narrow FOV Compton telescope surrounded by 24 shield counters made of BGO. The geometrical area of 525 cm^2 is currently assumed for the sum of 25 units. If we select an event that has two hits in the detector (and no hit in the BGO shields) and if we require the proper reconstruction for the Compton kinematics, the effective area at 200 keV becomes 100 cm^2 , including the reconstruction efficiency.

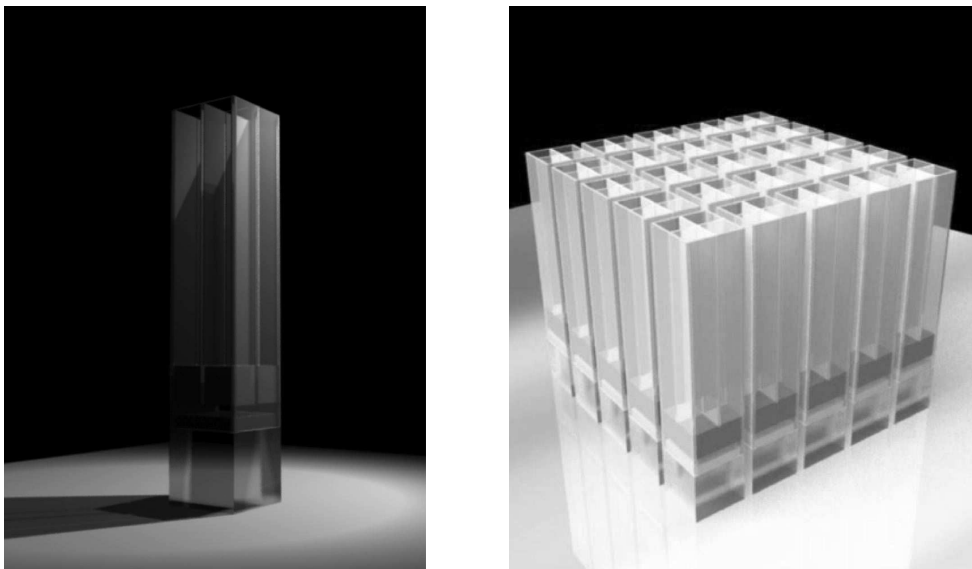


Figure 8. A artist drawing of the SGD for one unit (left) and 25 units (right). The side BGO shield is not shown.

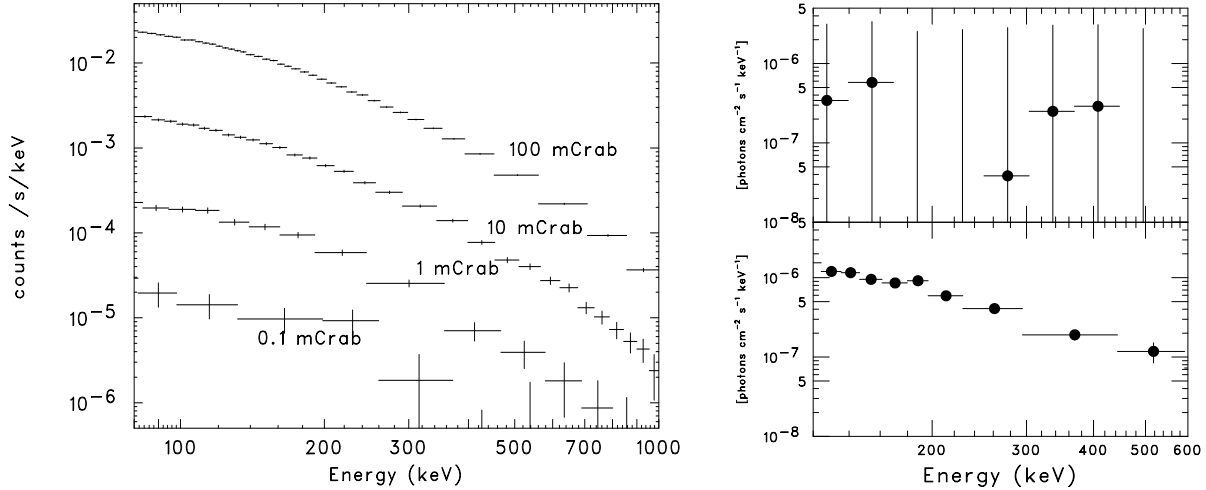


Figure 9. (left) Expected energy spectrum for a 100 ks observation of 0.1 – 100 mCrab sources with the Compton mode. The background level of 5×10^7 counts/s/cm²/keV is assumed. (right) Comparison of the energy spectrum for a 100 ks observation of 1 mCrab source expected from the SGD operated in the Compton mode (bottom plot) and the instrument with the effective area of 3300 cm² and the background level of 5×10^4 counts/s/cm²/keV (top plot). A systematic error of 5% is included in the background estimation for both cases.

The concept of a narrow FOV Compton telescope is expected to reduce drastically the background from radio-activation of the detector materials, which is a dominant background in the case of the Astro-E2 HXD.²⁵ Figure 9 (left) shows the expected energy spectrum for a 100 ks observation of 0.1 – 100 mCrab sources by the SGD with Compton mode, under an assumption of the background level of 5×10^7 counts/s/cm²/keV. Fig. 9 (right) compares the energy spectrum for a 100 ks observation of 1 mCrab source (photon index 1.7) expected from the SGD Compton mode (bottom plot) and that for an instrument with an effective area of 3300 cm² (50 times the SGD effective area) and a background level of 5×10^4 counts/s/cm²/keV. These results, derived from simple simulations, show that a high signal-to-background ratio is important to achieve the high sensitivity. In addition to the reduction of background, it should be noted that the 30' FOV of the one collimator is required to improve the sensitivity limited by source confusion below a few hundred keV. With the SGD, we can also measure polarization of incident gamma-rays from the azimuthal distribution of the Compton scattered photons.^{5,31}

Based on our CdTe and Si detector technologies, we are working on a Si/CdTe semiconductor Compton telescope. The photo of DSSD and CdTe pixel detectors used in the prototype and spectra taken from those detectors are shown in Fig. 10 and Fig. 11. Performance of the prototype and results of polarization measurements are described in other publications.^{18,30,32}

4. SUMMARY

The line and continuum sensitivities of the NeXT mission for 100 ks observation are shown in Fig.12 and Fig.13, together with those of other missions. The continuum sensitivity could reach several 10^8 photons/s/keV/cm² in the hard X-ray region and a few 10^7 photons/s/keV/cm² in the soft X-ray region. The high-energy response of the supermirror of NeXT will enable us to perform the first sensitive imaging observations up to 80 keV. By combining an X-ray CCD and a CdTe pixel detector, the WXI is an ideal solution for the focal plane detector of the supermirror, providing imaging capability and high spectral resolution with almost full detection efficiency. The narrow field-of-view Compton X-ray telescope realized by the SGD extends the bandpass to well above the cutoff for the hard X-ray telescope and allows us to study the high energy end of the particle spectrum through the sensitive observation of the X-ray spectrum up to 1 MeV. By combining these detectors, we expect to achieve an unprecedented level of sensitivity in the hard X-ray and sub-MeV X-ray region for both line and continuum emission.

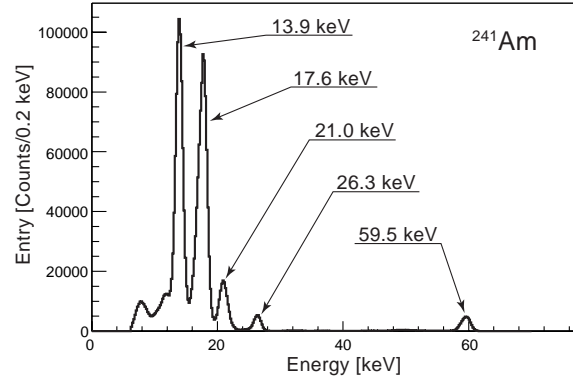
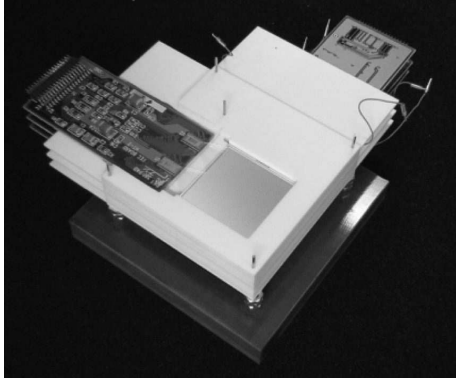


Figure 10. (left) Photo of three layers of DSSD stack developed for the prototype Si/CdTe Compton Camera^{30, 32} (right) Energy spectrum from DSSD for ²⁴¹Am source. The signal from each strip is processed by a newly developed analog front-end ASIC.²⁹ An energy resolution of 1.3 keV (FWHM) for 60 keV can be achieved at 0 °C.

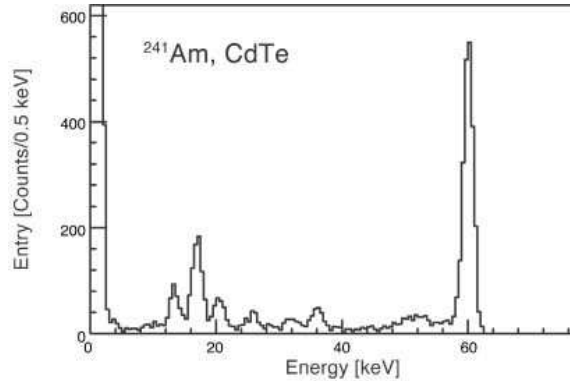
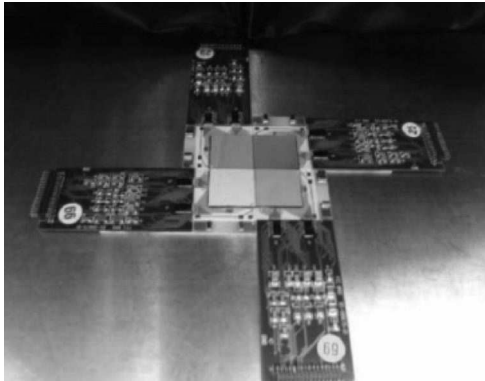


Figure 11. (left) Photo of large area CdTe pixel detectors developed for the prototype Si/CdTe Compton Camera.^{18, 31} The detector has an area of 3.2 cm × 3.2 cm and a thickness of 0.5 mm. Pixel size is 2 mm × 2 mm. (right) Energy spectrum from CdTe (one pixel) for ²⁴¹Am source. An energy resolution is 1.6 keV (FWHM) for 60 keV at 0 °C.

REFERENCES

1. NeXT Satellite Proposal, the NeXT working group, submitted to ISAS, 2003.
2. H. Kunieda, "Hard X-ray Telescope Mission (NeXT)," Proc. SPIE, vol. 5488, in press, 2004
3. T. Takahashi, T. Kamae, and K. Makishima, "Future Hard X-ray and Gamma-ray Observations." in New Century of X-ray Astronomy, ASP 251-210 (2002).
4. T. Takahashi, K. Nakazawa, T. Kamae, H. Tajima, Y. Fukazawa, M. Nomachi, and M. Kokubun, "High resolution CdTe detectors for the next generation multi-Compton gamma-ray telescope," Proc. SPIE, vol. 4851, pp. 1228-1235, 2002
5. H. Tajima, T. Mitani, T. Tanaka, H. Nakamura, T. Nakamoto, K. Nakazawa, T. Takahashi, Y. Fukazawa, T. Kamae, M. Kokubun, G. Madejski, D. Marlow, M. Nomachi, E. do Couto e Silva, "Gamma-ray polarimetry with Compton Telescope," Proc. SPIE, vol. 5488, in press, 2004
6. K. Mitsuda, "The soft x-ray spectrometer (SXS) on NeXT," Proc. SPIE, vol. 5488, in press, 2004
7. A. Furuzawa, T. Okajima, Y. Ogasaka, K. Tamura, Y. Tawara, K. Yamashita, "Design study of X-ray telescope onboard NeXT," Proc. SPIE, vol. 4851, 708, 2002
8. Y. Ogasaka, K. Tamura, R. Shibata, A. Furuzawa, T. Okajima, K. Yamashita, Y. Tawara, H. Kunieda, "NeXT Hard X-ray Telescope," Proc. SPIE, vol. 5488, in press, 2004

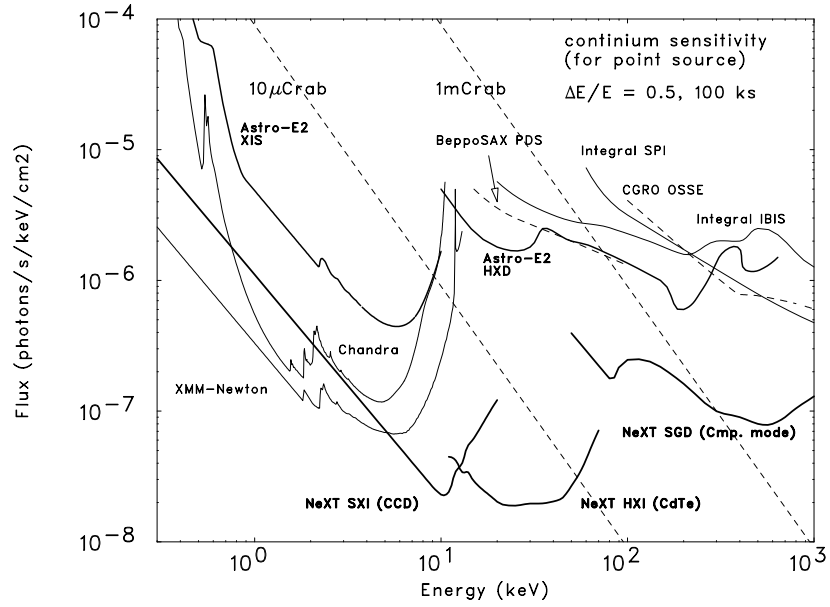


Figure 12. The expected W X I and SGD sensitivities for continuum emissions from a point source, assuming an observation time of 100 ks.

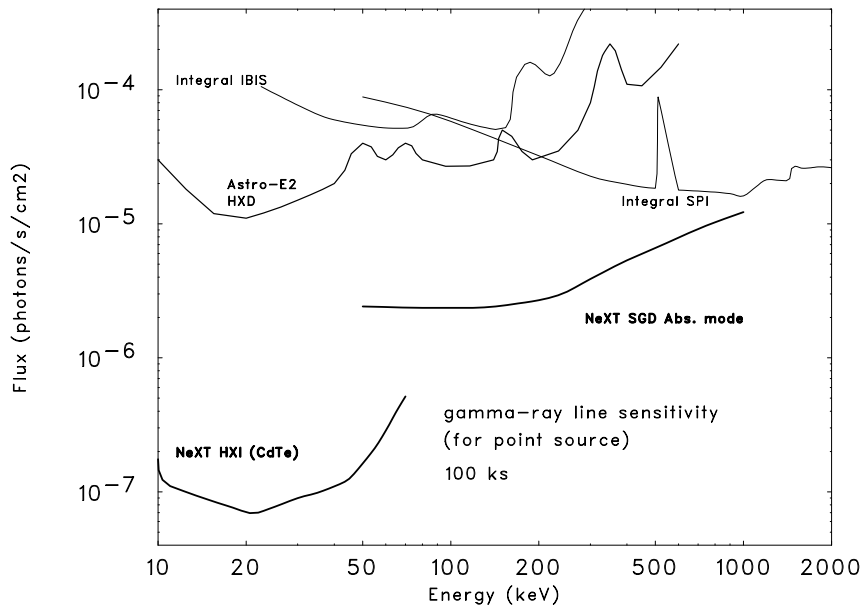


Figure 13. The expected W X I and SGD sensitivities for line emissions from a point source, assuming an observation time of 100 ks.

9. Y. Ogasaka et al., \Supermirror Hard X-ray Telescope and the results of first observation flight of InFOCUS," *Proc. SPIE*, vol. 4851, pp. 619-630, 2002
10. T. Takahashi, B. Paul, K. Hirose, C. Matsumoto, R. Ohno, T. Ozaki, K. Mori, Y. Tomita, \High-resolution Schottky CdTe Detectors for Hard X-ray and Gamma-ray Observations," *NIM A* 436 pp.111-119, 2000
11. T. Takahashi, K. Makishima, F. Fukazawa, M. Kokubun, K. Nakazawa, M. Nomachi, H. Tajima, M. Tashiro, and Y. Terada, \Hard X-ray and Gamma-ray detectors for the NeXT mission," *New Astronomy Reviews*, 48, pp. 309-313, 2004
12. T. Tsunui et al., \A Hybrid X-ray Imaging Spectrometer for NeXT and the Next Generation X-ray Satellite", *Adv. Space Res.*, in press.
13. E. Miyata, C. Natsukari, T. Kamazuka, H. Kouno, H. Tsunemi, M. Matsuoka, H. Tomida, S. Ueno, K. Hamaguchi, I. Tanaka \Developments of CCDs and relevant electronics for the X-ray CCD camera of the MAXI experiment onboard the International Space Station," *Proc. SPIE*, vol. 4497, pp. 11-18, 2002
14. S. Takagi, T. G. Tsunui, H. Matsumoto, K. Koyama, H. Tsunemi, E. Miyata, S. Miyazaki, Y. Kamata, \The development of back supportless CCDs and wideband hybrid x-ray imager for the NeXT Satellite," *Proc. SPIE*, vol. 5501, in press, 2004
15. T. Takahashi and S. Watanabe \Recent Progress on CdTe and CdZnTe detectors," *IEEE Trans. Nucl. Sci.*, vol. 48, pp. 950-959, 2001
16. T. Takahashi et al., \High Resolution Schottky CdTe Diodes," *IEEE Trans. Nucl. Sci.*, 49, No. 3, pp. 1297-1303, 2002
17. K. Nakazawa et al. \Improvement of the CdTe Diode Detectors using a Guard-ring Electrode," *IEEE Trans. Nucl. Sci.*, in press, 2004
18. T. Tanaka et al., \Development of a Si/CdTe semiconductor Compton Telescope," *Proc. SPIE*, vol. 5501, in press, 2004
19. K. Onuki, H. Inoue, K. Nakazawa, T. Mitani, T. Tanaka, T. Takahashi, C. M. H. Chen, W. R. Cook, F. A. Harrison, \Development of Uniform CdTe Pixel Detectors Based on Caltech ASIC," *Proc. SPIE*, vol. 5501, in press 2004
20. T. Kamae et al., \Well-type Phoswich Counters for Low-Flux X-Ray/Gamma-ray Detection," *Proc. SPIE*, vol. 1734, pp. 2-13, 1992
21. T. Takahashi et al., \Newly Developed Low Background Hard X-ray/Gamma-ray Telescope with the Well-type Phoswich Counters," *IEEE Trans. Nucl. Sci.* 40, pp. 890-898, 1993
22. T. Kamae et al., \Astro-E hard X-ray detector," *Proc. SPIE*, vol. 2806, pp. 314-328, 1996
23. M. Tashiro et al. \Performance of the ASTRO-E Hard X-ray Detector," *IEEE Trans. Nucl. Sci.* 49, pp. 1893-1897, 2002
24. K. Makishima, et al., \The HXD-II on ASTRO-E-II: Another Challenge to the Hard X-ray Sky," in *New Century of X-ray Astronomy*, *ASP*, pp. 251-252, 2002
25. M. Kokubun et al., \Improvements of the Astro-E2 Hard X-ray Detector (HXD-II)," *IEEE Trans. Nucl. Sci.*, in press, 2004
26. M. Kawaharada et al., \Development and calibration of HXD-II onboard Astro-E2," *Proc. SPIE*, vol. 5501, in press 2004
27. J. Kataoka et al., \Performance of the most recent avalanche photodiodes for future x-ray and gamma-ray astronomy," *Proc. SPIE*, vol. 5501, in press, 2004
28. T. Nakamoto, Y. Fukazawa, T. Ohnogi, T. Kamae, and J. Kataoka, \BGO readout with photodiodes as a soft gamma-ray detector at 30 C," *NIM A*, in press, 2004
29. H. Tajima et al. \Performance of a low noise front-end ASIC for Si/CdTe detectors in Compton gamma-ray telescope," *IEEE Trans. Nucl. Sci.*, in press, 2004
30. H. Tajima, T. Kamae, S. Uno, T. Nakamoto, Y. Fukazawa, T. Mitani, T. Takahashi, K. Nakazawa, Y. Okada, and M. Nomachi, \Low noise double-sided silicon strip detector for multiple-Compton gamma-ray telescope," *Proc. SPIE*, vol. 4851, pp. 875-884, 2002
31. T. Mitani et al., \A Prototype Si/CdTe Compton Camera and the Polarization Measurement," *IEEE Trans. Nucl. Sci.*, in press, 2004
32. Y. Fukazawa et al., \Low-noise double-sided silicon strip detector for soft gamma-ray Compton camera," *Proc. SPIE*, vol. 5501, in press, 2004